2004

NASA FACULTY FELLOWSHIP PROGRAM

MARSHALL SPACE FLIGHT CENTER

THE UNIVERSITY OF ALABAMA
THE UNIVERSITY OF ALABAMA IN HUNTSVILLE
ALABAMA A&M UNIVERSITY

ENHANCEMENT AND ANALYSIS OF REAL-TIME RADIOGRAPHY IMAGES

Prepared By:	Dr. Edward R. Doering
Academic Rank:	Associate Professor
Institution and Department:	Rose-Hulman Institute of Technology Electrical and Computer Engineering
NASA/MSFC Directorate:	Engineering (ED32)
MSFC Colleague:	Dr. Sam Russell

Introduction

Shuttle Redesigned Solid Rocket Motor (RSRM) nozzle interiors fabricated from carbon phenolic composite exhibit "ply lift" when hot fired. The composite surface is smooth when fabricated, but the individual plies separate and lift away from the surface when exposed to high-temperature and high-pressure exhaust gas. Figure 1 shows a cross section of a post-fired composite in which ply lift is evident as dark fissures. Surface charring is also visible as a darker band about 0.2 inches thick. Charring is normal, but ply lift is not desirable since the fissures could possibly initiate an abnormal exhaust path from the RSRM. The underlying mechanisms of ply lift are under investigation as part of the Shuttle Return-To-Flight Program.

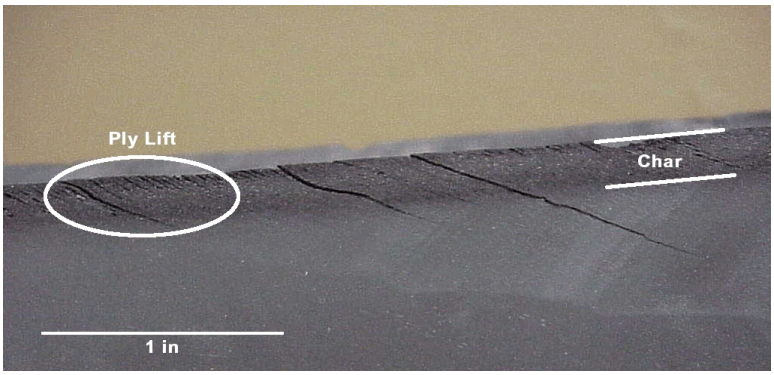

Figure 1: Cross section of post-fired carbon phenolic composite.

Subscale solid rocket motors are used as a cost-effective way to simulate actual hot firing of the RSRM. The Solid Fuel Torch (SFT) subscale motor is specifically designed to evaluate RSRM materials. The output of the SFT is channeled through a convergent cone fabricated from carbon phenolic composite. Real-time radiography (RTR) of the cone interior during hot firing permits direct observation of ply lift dynamics over time, thereby providing information to validate analytical models of the ply lift process. Key information to extract from the image sequence includes:

1. time when ply lift is first detectable,
2. minimum detectable length of the ply lift crack,
3. charring depth over time,
4. charring depth as a function of position along the cone, and
5. lift height over time.

The RTR setup was optimized to minimize geometric unsharpness and to maximize contrast. The ply lift and charring processes are visible to experienced radiographers, but photon counting noise and low contrast obscure the ply lift indications for the casual observer. Moreover, quantitative measurement of phenomena such as charring depth versus time would be tedious if done manually, since the typical RTR image sequence is 300 to 400 frames long. Thus, the goals of this project are two-fold:

1. Enhance the RTR image sequence to facilitate human interpretation, and

2. Analyze the RTR image sequence to extract quantitative information such as ply lift height as a function of time.

Enhancement of RTR Image Sequence

A Pantak X-ray source and a Varian 2520 flat panel amorphous silicon detector image the cone's interior. The source operates at 160 kVp and 4 mA. Frames are captured at approximately 8 frames per second, with a total sequence length of 30 to 40 seconds. Figure 2 shows a frame from the post-fire image, where crack-like lines indicate ply lift and the band of lighter intensity indicates charring and ply lift. Pressure and temperature sensors and associated wiring are visible in the center of the cone.

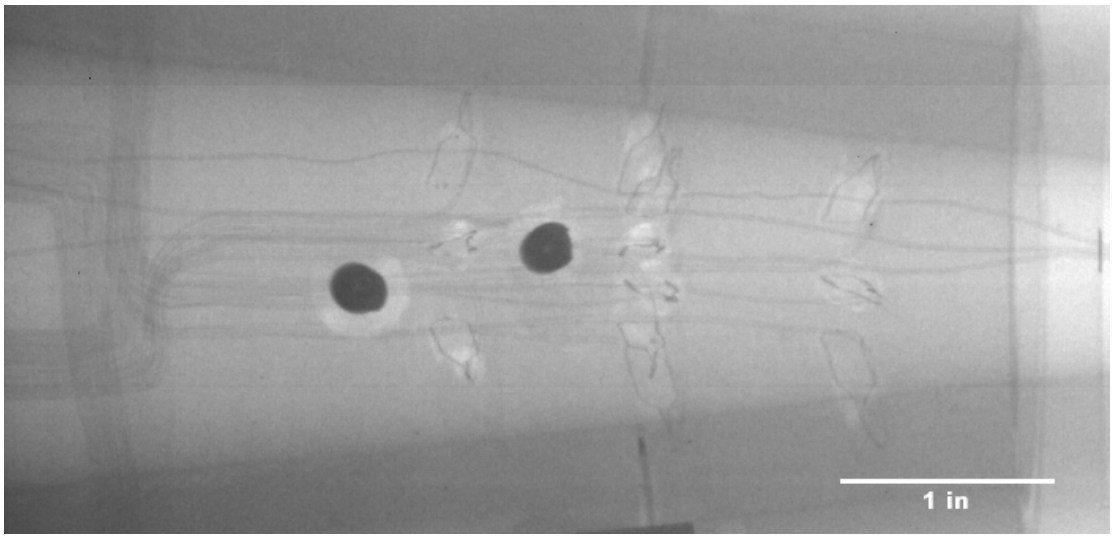

Figure 2: RTR image of cone interior.

The X-ray source intensity fluctuates somewhat, causing a global variation in the mean value of each frame. A region of interest (ROI) was selected at the edge of the image away from the ply lift and charring region. The mean value of the ROI was found and subtracted on a frame-by-frame basis. Removing this fluctuation reduces visual flicker in the final contrast-enhance image, and also improves reliability of intensity thresholding-based feature detection.

Frames are captured in "raw mode" to maximize the frame rate flat panel detector, so darkfield correction must be applied as a post-processing step. Frames acquired after the X-ray source was shut off are averaged to estimate the fixed-pattern noise of the detector. This "darkfield" image is subtracted from all frames before further processing.

Photon counting noise is reduced using a running average of four frames, equivalent to a time window of 0.5 seconds duration. Image signal-to-noise ratio increases by $\sqrt{N}$, where N is the number of frames, but temporal blurring also increases with increased frames. Four frames were selected to balance noise reduction against temporal blurring.
Image subtraction is used to highlight any differences that appear after hot firing begins. Frames captured just before firing were averaged to minimize noise and used as the reference

background image, which is subtracted from each frame in the sequence. Figure 3 shows the resulting difference image after contrast stretching, with the plylift cracks and charring region now clearly evident.

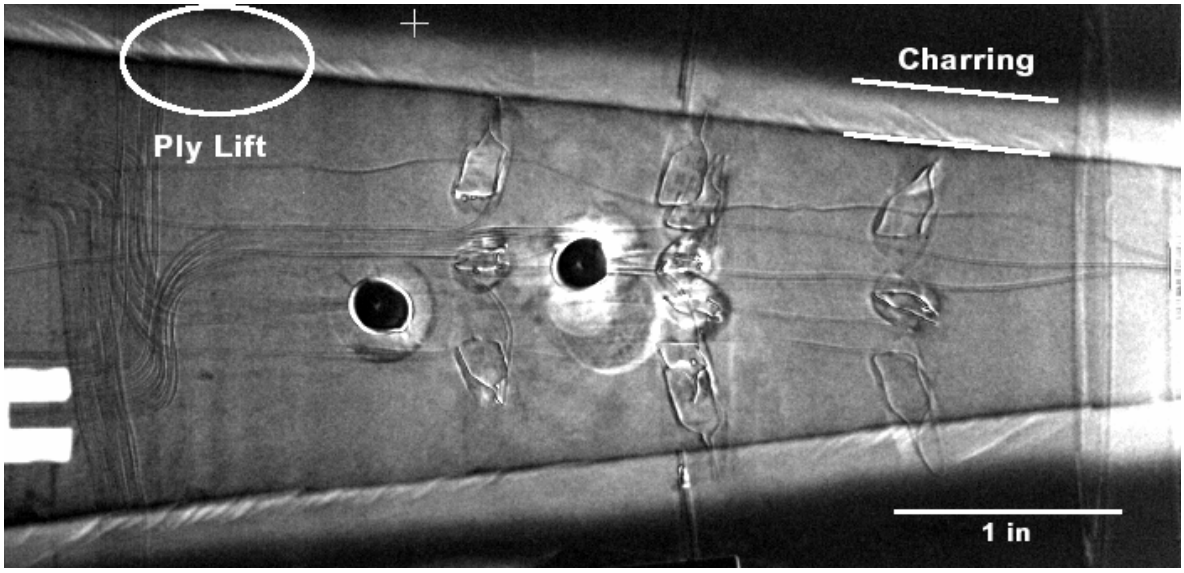

Figure 3: Enhanced RTR image showing ply lift and charring

Analysis of RTR Image Sequence

The first frame of the difference sequence is a zero-mean Gaussian noise field with standard deviation of σ intensity levels. Thresholding the image at $+9\sigma$ clearly delineates the plylift cracks, while thresholding at $+2\sigma$ shows the charring. The interior edge of the convergent cone becomes detectable at two seconds.

The charring region was isolated by rotating to correct for the angle of the interior cone boundary, cropping the image, and thresholding to create a binary image. The thickness of the charring region can then be observed as a function of position in the cone and as a function of time. Figure 4(a) plots the boundary position as a function of time.

The intensity of the cone interior gradually increases with time which indicates a reduction in the mass attenuation coefficient of the material. Figure 4(b) plots the intensity normalized to the starting value. The plots in Figure 4 show a similar trend, indicating that perhaps either measurement technique could be used to estimate char depth.

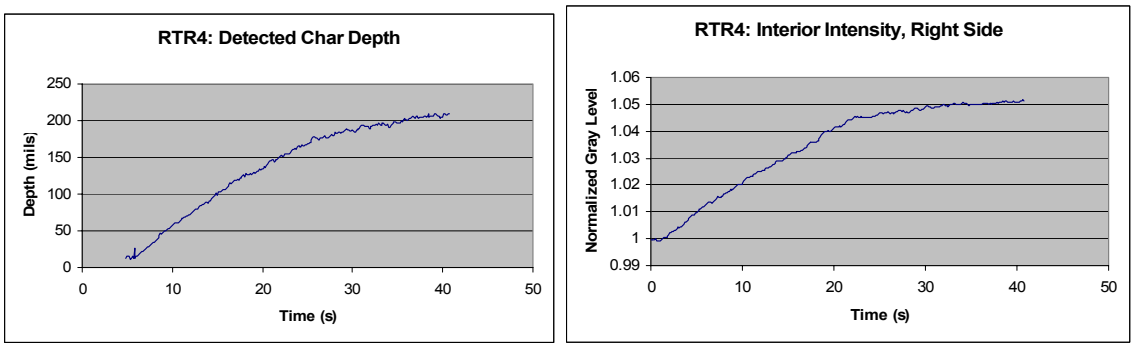

Figure 4: Char depth versus time for (a) edge tracking and (b) intensity increase.

The ply lift boundaries on the cone interior wall were isolated by an edge tracking algorithm, and the total reduction of the cone's inner diameter over time was measured. Dividing by two yield the average ply lift height as plotted in Figure 5. The reduction begins at 2 seconds, and then increases quickly to a plateau at 15 seconds. The ply lift process is noticeably more abrupt in comparison to the charring depth plots of Figure 4.

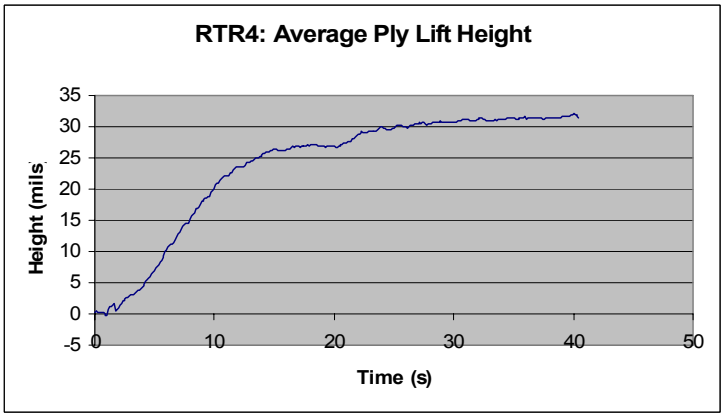

Figure 5: Average ply lift height versus time.

Conclusion

Real-time radiography has been demonstrated as an effective way to observe ply lift dynamics during hot firing. A series of corrective techniques for X-ray tube intensity fluctuation, detector fixed-pattern noise, and photon counting noise followed by background subtraction and contrast enhancement yield an image sequence that is enhanced for human interpretation. Automated analysis by edge tracking allows ply lift dynamics such as lift height and charring depth to be quantified over time.

Acknowledgements

The author would like to thank Ron Beshears and Sam Russell for their on-going support, as well as the entire team of engineers and technicians in the Nondestructive Evaluation and Tribology Group of the Marshall Space Flight Center's Engineering Directorate.